

EFFECTS OF VARIOUS NUCLEATION AGENTS ON CRYSTALLIZATION KINETIC OF LAS GLASS CERAMIC

M. Rezvani

* *m_rezvani@tabrizu.ac.ir*

Received: March 2011

Accepted: November 2011

Department of Materials Engineering, Faculty of Mechanical Engineering, University of Tabriz, Tabriz, Iran.

The effect of Y_2O_3 , CeO_2 , P_2O_5 , ZrO_2 and TiO_2 in single, double and triple form on crystallization mechanism of $Li_2O-Al_2O_3-SiO_2$ (LAS) glass-ceramic system was investigated. The nucleation and crystallization peak temperatures of optimized samples in each group were determined by Ray & Day method. The crystalline phase was determined by the X-ray diffractometry. The micro-structure of the samples was studied by SEM technique. Crystallization activation energy, E , and kinetic constants (n , m) were determined by differential thermal analysis (DTA) through Marotta and Augis-Bennet methods. According to the results, the Avrami constants (m , n) derived from the Marotta and Augis-Bennett, glasses containing both ZrO_2 and TiO_2 nuclei were showed bulk crystallization. The crystallization mechanism of specimens containing ZrO_2 , TiO_2 and CeO_2 in the triple nuclei series represent two-dimensional bulk crystallization. By comparison of Avrami constants and activation energy of crystallization of optimized samples with other results they gave much lower value of E (255.5 kJ/mol) and higher value of n in 4.38. The lattice constants of the main phase (β -eucryptite solid solution) in samples were determined according to the XRD results.

Key words: LAS glass ceramics, Eucryptite, h-quartz, Kinetic parameters, Crystallization mechanism.

1. INTRODUCTION

Glass-ceramic materials are produced via the controlled crystallization of glass that involves a two stage heat treatment, namely a nucleation and a crystallization stage have some advantages in comparison with ceramics that are produced via powder metallurgy such as minimal or even zero porosity and homogeneous microstructure [1]. The aim of combining the aforementioned properties achieved by precipitating a large volume percent of the desired crystal phases (at least 50% vol.) in the glass-ceramic [2].

Lithium aluminum silicate (LAS) glass-ceramics, one of the most important glass-ceramic systems, has been extensively investigated and commercialized because of its low, zero or negative thermal expansion coefficient as well as excellent thermal and chemical durability [3-10].

The most important stable crystalline phases in the LAS glass-ceramics system is Eucryptite, Spodumene, Petalite and metastable solid solution i.e. α -quartz (h-quartz) and Kitite (tetragonal SiO_2) [1].

The most effective nucleation agents in this system are TiO_2 , ZrO_2 , Fe_2O_3 , Cr_2O_3 , NiO , ZnO , V_2O_5 , P_2O_5 and Ta_2O_5 . The investigation showed

that TiO_2 , ZrO_2 and P_2O_5 are more effective nucleating agents for crystallization of above-mentioned glass-ceramics [11].

Sung et al. [12] introduced TiO_2 as effective nucleant in $Li_2O-Al_2O_3-SiO_2$ glass-ceramic system. According to their results the activation energy for crystallization of a specimen containing 3.85 wt% TiO_2 was 299. The Avrami constant, n , and the activation energy for crystallization of samples containing a combination of TiO_2 and ZrO_2 nuclei were also determined by M. Guedes et al. [13] respectively as 1 to 3 and 132 to 195.8. Min [14], Hu and co-workers [15] reported activation energy were ranged from 303 to 425 and Avrami constant is 2.8 with the same nuclei. Zheng et al. [16] showed an activation energy of 512 for crystallization of a specimen containing TiO_2 (2.3 wt%), ZrO_2 (2 wt%) and Y_2O_3 (4.46 wt%). There are different methods such as Marotta, Matusita, Modified Kissinger and Augis-Bennett for determining the crystallization mechanism in glass-ceramics. The crystallization capability of glass specimens is dependent on crystallization deriving force and crystallization activation energy, and it increases with increase of crystallization deriving force and reduction of crystallization activation energy [17-19]. In the present work the crystallization

mechanism and activation energy for crystallization of glasses in $\text{Li}_2\text{O}-\text{Al}_2\text{O}_3-\text{SiO}_2$ system, containing a mixture of TiO_2 , ZrO_2 , P_2O_5 , CeO_2 and Y_2O_3 (in the single, double and triple nuclei series) were investigated by using various methods using differential thermal analysis(DTA).

2. EXPERIMENTAL PROCEDURE

The base glass composition (S) and other compositions are presented in table 1. Nucleation agents i.e. Y_2O_3 , CeO_2 , P_2O_5 , ZrO_2 and TiO_2 were added to sample S in different combinations. The raw materials used were reagent grade $\alpha\text{-Al}_2\text{O}_3$ (PB-502 Alumina, Martinswerk company, $d_{50}<45$), SiO_2 (Hamedan silica with purity up to 99%, $d_{50}<45$), Li_2CO_3 (Merck-No.105671), NaCO_3 (Merck-No.106398), K_2CO_3 (Merck-No.103924), $\text{Mg}(\text{OH})_2$ (Merck-No.5870), ZnO (Merck-No.102075), TiO_2 (Merck-No.808), ZrO_2 (Merck-No.8614), P_2O_5 (Merck-No.540), Y_2O_3 (Merck-No.2590) and CeO_2 (Merck-No.2283). The mixture of raw materials after mixing thoroughly were transferred to an alumina crucible and melted at 1650°C for 2hours in an electric furnace (AZAR-F3-1720). Then, the melts were cast in pre-heated stainless steel molds and cooled naturally to the room temperature. The thermal behavior of glass samples monitored by DTA technique was carried out using a simultaneous thermal analyzer (DTG-60 AH Shimadzu). Nucleation temperature (T_n), crystallization peak temperature (T_p) and glass transformation temperature (T_g), activation energy of crystallization, Avrami constant (n) and kinetic constant(m) were determined by DTA

results of the specimens. The reference material in these experiments was $\text{-Al}_2\text{O}_3$ powders and the heating rates used was 10.5,12.5,15 and $17.5^\circ\text{C}/\text{min}$. Dilatometric softening points (T_d) and coefficient of thermal expansion (TEC) was also measured by dilatometer (model E-402 Netzsch). The optimum nucleation temperature of the glass was determined by the Ray & Day method[20]. Micro-hardness of polished glass and glass-ceramic was measured by a Vickers micro-hardness tester (Leitz GMBH D-6630 Wetzlar) with an indentation of 50gf for 30 seconds. The average value was obtained from measurement of 10 indentations. The three point bending strength of the glasses and glass ceramics were determined using a universal testing machine (Instron Universal Testing 1196), with loading rate of $0.5\text{ mm}/\text{min}$ and based on the ASTM C 158-84. Five polished rectangular specimens ($40 \times 5 \times 5\text{ mm}$) were tested for each composition. The bulk density of the samples were also measured by the Archimedes method. X-ray diffraction (XRD) was used in order to identify the crystallization products in the heat-treated specimens (Siemons-D500). Cu- $k\alpha$ radiation was used at 20 kV setting and in the 2θ range of $10-70^\circ$. The samples after polishing and etching in 5%HF solution for 30 seconds were coated with a thin film of gold and subjected to SEM examination (scanning electron microscope, LEO 440i). The lattice parameters of the hexagonal β -eucryptite solid solution have been determined by the following formula[7]:

$$d_{hkl}^2 = \frac{a^2}{\frac{4}{3}(h^2 + hk + k^2) + l^2 \frac{a^2}{c^2}}$$

Table1. Chemical composition of glasses

| Specimen | Base Glass (wt %) | | | | | | | Nucleation Agents (wt %) | | | |
|-----------------------------------|-------------------|-------------------------|-----------------------|-----------------------|----------------------|--------------|--------------|--------------------------|----------------|------------------------|----------------|
| | SiO_2 | Al_2O_3 | Li_2O | Na_2O | K_2O | MgO | ZnO | TiO_2 | ZrO_2 | Y_2O_3 | CeO_2 |
| S | 66.4 | 23.04 | 5.2 | 0.17 | 0.17 | 2.08 | 2.08 | - | - | - | - |
| ST_3 | | | | | | | | - | - | - | - |
| ST_3Z_1 | | | | | | | | 3 | 1 | - | - |
| $\text{ST}_3\text{Z}_1\text{Y}_1$ | | | | | | | | | | 1 | - |
| $\text{ST}_3\text{Z}_1\text{C}_3$ | | | | | | | | | | - | 3 |

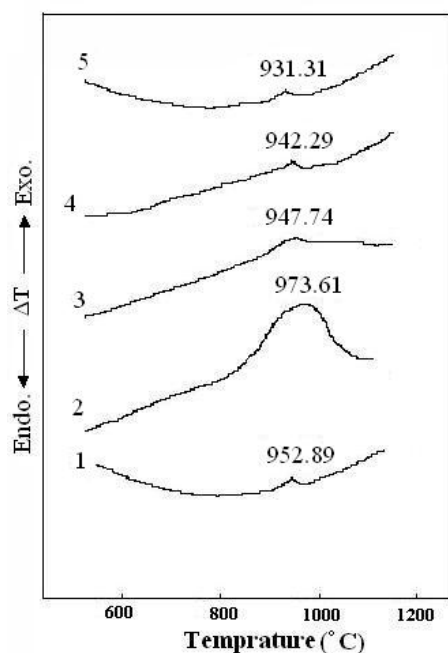


Fig. 1. DTA curves of the glasses S(1), SZ1(2), SZ2(3), SZ3(4) and SZ4(5) at the heating rate of 10 °C/min

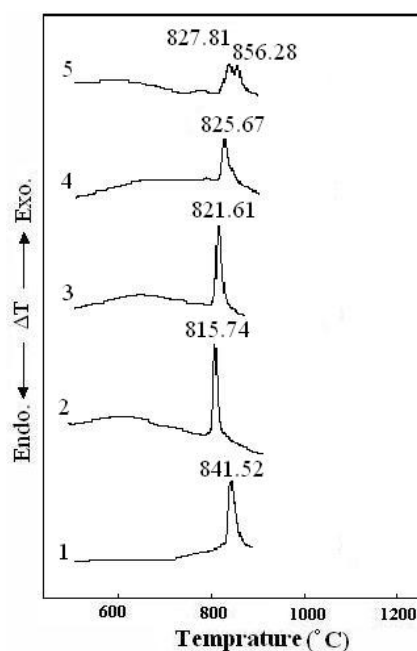


Fig 2. DTA curves of the glasses (1) ST_3 (2) ST_3Z_1 (3) ST_3Z_2 (4) ST_3Z_3 and (5) ST_3Z_4 at the heating rate of 10 °C/min

3. RESULTS AND DISCUSSION

Table 1 shows the chemical composition of some of prepared samples. In this table the base glass composition was labeled as S. In order to investigate the effect of type and amount of effective nuclei different nuclei were added to the base S glass composition. Fig 1 represents DTA curves of specimens containing various amounts of ZrO_2 . It can be seen that only one exothermic peak was observed in each curve which is associate with precipitation of a stuffed β -quartz solid solution (h-quartz). It can be seen that the specimen containing 1wt.% ZrO_2 was the most promising specimen exhibiting the highest and sharpest DTA peaks with the lowest temperatures in this series. The sharpness of exo-peak reduced gradually with increasing the amount of ZrO_2 .

According to the DTA results, TiO_2 is more effective than ZrO_2 because of its high ionic field strength that enhances the phase separation and improve the heterogeneous nucleating rate. The presence of ZrO_2 , increases the viscosity of the melt and also increases the activation energy of the crystallization that shift the peak temperature

up to high values. Investigating the DTA curves of optimized specimens containing single nucleating agent (ZrO_2 , TiO_2 , P_2O_5 , Y_2O_3 and CeO_2) represents that ST_3 (3Wt.% TiO_2) is the best composition. ZrO_2 , P_2O_5 , Y_2O_3 and CeO_2 were added to ST_3 (1-4 wt.%). According to the DTA patterns, TiO_2 along with ZrO_2 as nucleating agent in the S glass composition, ST_3Z (3wt.% TiO_2 and 1wt.% ZrO_2), was more appropriate than other samples. As it can be seen in Fig 2, the crystallization peak temperature was reduced from 841°C (ST_3) to 815°C (ST_3Z), but increasing of ZrO_2 decreases the crystallization peak intensity. Presence of TiO_2 and ZrO_2 additives, causes the phase separation of the base glass and formation of the $Al_2Ti_2O_7$ phase in SiO_2 -poor regions [21,22].

The presence of ZrO_2 as the nucleating agent increases the viscosity and encourage the formation of β -spodumene [22]. Two peaks can be seen in ST_3Z_4 specimen, the first one refers to the formation of h-quartz and the second refers to the transformation of h-quartz to β -spodumene [23,24]. The bulk nucleating rate in the presence of both TiO_2 and ZrO_2 additives were increased

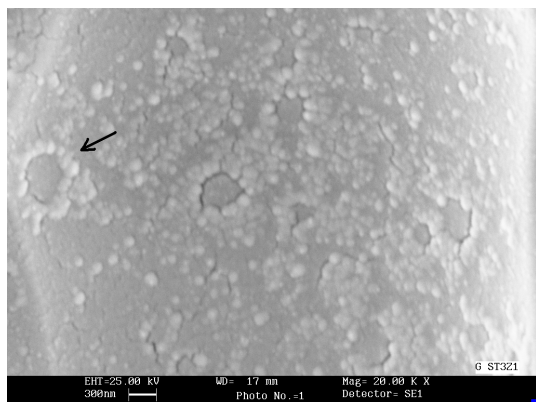


Fig 3. SEM micrograph of ST_3Z_1 glass that represents the separated regions in glass matrix

and the uniform crystallization phase was obtained[25]. Hsu et al.[23] introduced that TiO_2 and ZrO_2 precipitate as $ZrTiO_4$ in the SiO_2 -poor regions phase separated and act as nucleating agent. Fig. 3 represent the phase separation in ST_3Z glass.

According to results addition of 1wt% Y_2O_3 (ST_3ZY_1) and 3 3wt.% CeO_2 (ST_3ZC_3) to the specimen ST_3Z_1 provided better bulk nucleation and crystallization. P_2O_5 and CeO_2 were also added to ST_3ZY_1 and ST_3ZC_3 (1-4wt.%) . In the both cases crystallization peak temperature were increased (above 900 °C). The sharpness of exo-

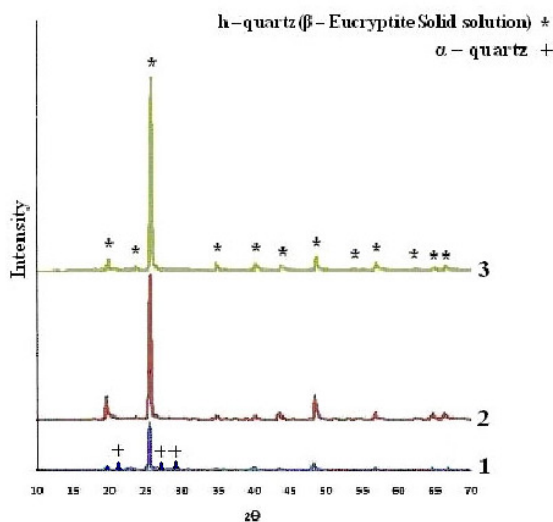


Fig 3. SEM micrograph of ST_3Z glass that represents the separated regions in glass matrix

peaks gradually decreased and eventually the peak vanished, therefore the specimens containing four nucleating agents were not appropriate.

Fig.4 represent the XRD patterns of three optimized samples after heat treatment at their DTA peak crystallization temperature for 3h. As it can be seen the main crystalline phase in these specimens is h- quartz (JCODS 70-1580). For the ST_3ZC_3 specimen, in addition to main phase, the free quartz and h-quartz can be seen. Formation of free quartz causes non-appropriate CTE and thermal shock resistance.

The most suitable nucleation temperature was determined by the Ray and Day method. The samples were first heated for 3 hours at several temperatures (between T_g and crystallization peak onset) i.e. 600 to 735 °C for ST_3Z , 680 to 740 °C for ST_3ZY_1 and 650-754 °C for ST_3ZC_3 .

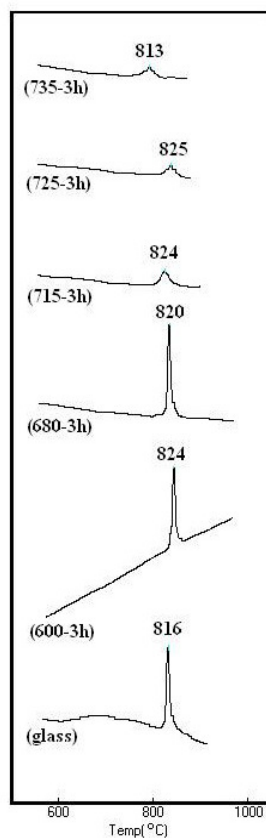


Fig 5. DTA plots of the ST_3Z glass heat treated at different temperatures with soaking time for 3 hours (in order to determine the nucleation temperature)

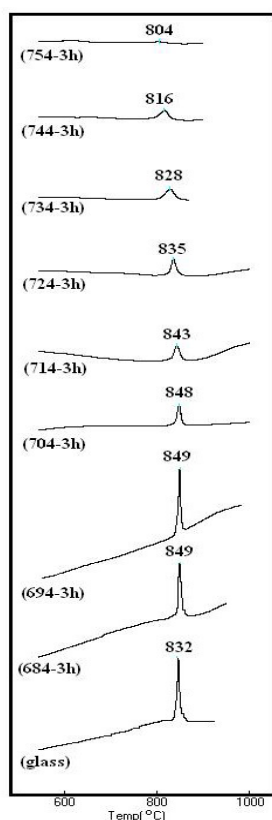


Fig 6. DTA plots of the ST_3ZY_1 glass heat treated at different temperatures with soaking

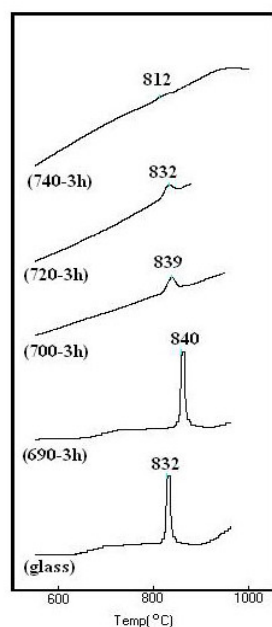


Fig 7. DTA plots of the ST_3ZC_3 glass heat treated at different temperatures with soaking time for 3 hours

Table 2. Unit-cell dimension for optimum samples and various h-quartz type alumina-silicates

| composition | Lattice constants ($^{\circ}A$) | |
|---------------------|-----------------------------------|-------|
| | a | c |
| ST_3Z | 5.200 | 5.434 |
| $ST_3Z Y_1$ | 5.221 | 5.661 |
| $ST_3Z C_3$ | 5.208 | 5.850 |
| $LiAlSi_2O_6$ | 5.212 | 5.457 |
| $Zn_{0.5}AlSi_2O_6$ | 5.220 | 5.460 |

Then the DTA test was performed. The results were shown in figures 5 to 7. According to this method optimum nucleation temperature was 680, 694 and 694 respectively. The lattice parameters of β -eucryptite solid solution have been calculated from the measured d-value of crystal plane with the expression relative to the hexagonal crystal system. The crystal planes (101), (112) and (100) have been selected for determination of lattice parameters. The 2θ values were used 25.259, 47.534 and 19.542. Table 2 shows the lattice parameters for optimized specimens.

These results are comparable with lattice constants of h-quartz-type and keatite-type aluminosilicates ($Zn_{0.5}AlSi_2O_6$, and $LiAlSi_2O_6$ composition) [21].

Fig. 8 and 9 show the results of variation of $\ln \alpha$ vs. $1/T_p$ and $\ln \Delta T$ vs. $1/T$ for specimen ST_3ZY_1 derived from the Marotta's method [17,27& 28]:

$$\begin{cases} \ln \Delta T = \frac{-nE}{RT} + const. \\ \ln \alpha = \frac{-E}{RT_p} + const. \end{cases} \quad (\text{Marotta equations})$$

Where α , T_p , E , R , n and ΔT indicates the heating rate, crystallization peak temperature, activation energy, gas constant and the value of Avrami constant and deviation from the baseline respectively.

The plot of both patterns is expected to be



Fig 8. Variation of $\ln \alpha$ vs $\frac{1}{T_p}$ in $\text{ST}_3\text{Z}_1\text{Y}_1$ for determination of the crystallization activation energy according to Marotta method

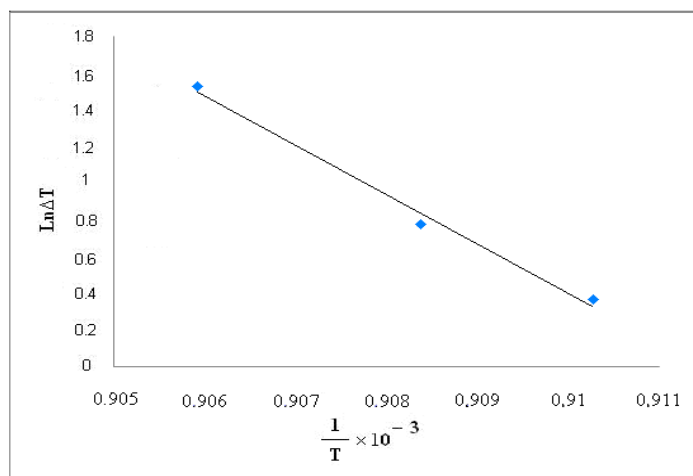


Fig 9. Variation of $\ln \Delta T$ vs $\frac{1}{T}$ in ST_3ZY_1 for determination of the Avrami exponent according to Marotta method

linear, and value of E and n can be derived from the slope of two lines, respectively.

The crystallization kinetic characteristics of optimized samples can be decided as follows by Augis-Bennett which is expressed as:

$$\begin{cases} \ln \frac{T_p^2}{\alpha} = \frac{E}{RT_p} + \text{const.} \\ n = \frac{2.5}{\Delta T} \times \frac{RT_p^2}{E} \end{cases} \quad (\text{Augis-Bennett equations})$$

In this equation ΔT is the width of the exothermic peak at the half maximum intensity. The value of n close to 1 means that surface crystallization dominates overall crystallization, while the value of n close to 2 means that one-

dimensional crystallization, the value of $n=3$ implies a two-dimensional bulk crystallization process and the value of $n=4$ implies a three-dimensional bulk crystallization process [26].

The plots of $\ln \frac{T_p^2}{\alpha}$ vs. $1/T_p$ was showed in fig. 10 to calculate the activation energy and Avrami constant, n .

Table 3 summarizes the crystallization activation energy and the Avrami constant determined by the two above-mentioned methods for optimized samples. It can be deduced that the n values determined from the Marotta and Augis-Bennett methods are more or less identical. Considering the amount of the Avrami constants calculated for optimized samples, it can be



Fig 10. The plots of $\ln \frac{T_p^2}{\alpha}$ vs. $1/T_p$ for ST_3ZY_1 for determination of the crystallization activation energy according to Augis-Bennett method

Table 3. Avrami exponent and crystallization activation energy determined by various methods

| Composition | Avrami constant (<i>n</i>) | | Activation energy (E) (kJ/mol) | |
|----------------------------------|------------------------------|---------------|-----------------------------------|---------------|
| | Marotta | Augis-Bennett | Marotta | Augis-Bennett |
| ST ₃ Z | 4.23 | 4.38 | 269.11 | 255.2 |
| ST ₃ Z Y ₁ | 3.70 | 3.81 | 287.8 | 273.39 |
| ST ₃ Z C ₃ | 2.96 | 3.03 | 365.6 | 349.67 |

deduced that in ST₃Z and ST₃ZY₁ with *n* value of approximate 4, the crystallization mechanism were three-dimensional and indicates homogeneous crystallization. Therefore the shape of the crystalline particles in these samples are spherical. The comparison of *E* values of ST₃Z and ST₃ZY₁ glasses indicates the same crystallization mechanism predominates in both glasses. However, it can be seen that the added Y₂O₃ increased the activation energy of the crystallization. This issue would probably lead to reducing of crystallization rate of ST₃ZY₁ glass. The comparison of *n* and *E* values of ST₃Z and ST₃ZC₃ glasses, it can be seen that the added CeO₂ increased the activation energy of crystallization. Therefore, considering the amounts of the Avrami constants calculated from the Marotta and Augis-Bennett methods in

ST₃ZC₃ specimen the crystallization mechanism was two-dimensional bulk type and the shape of the particles are plate like. It should be noted that in spite of the high value of *n*, the *E* value determined in this investigation was the lowest reported for this system [27].

Fig.11 shows the SEM micrograph of ST₃ZY₁ and ST₃ZC₃ glass ceramics have been nucleated and crystallized in their optimized *T_n* and *T_p* for 3 hours. The presence of platelet crystalline particles and spherical crystalline particles in the microstructure of ST₃ZC₃ and ST₃ZY₁, respectively, is again an evidence for a two dimensional and three-dimensional crystallization in these samples. As it can be seen, the precipitated crystalline particles of ST₃ZY₁ are smaller than 300 nm and ST₃ZC₃ particles are bigger than 1 μm. It seems the fine texture of

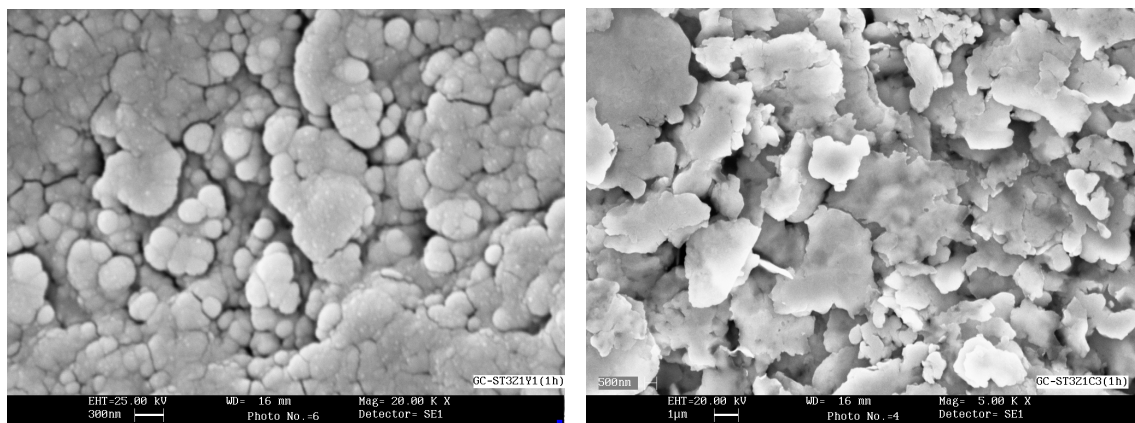


Fig 11. SEM micrograph of (a) $ST_3Z_1Y_1$ and (b) $ST_3Z_1C_3$ nucleated and crystallized at T_n and T_p

ST_3ZY_1 which is organized from a suitable nucleating agent has led to a high bending strength in this sample. According to above-mentioned discussion these glass-ceramics can be used as high thermal shock resistance products for commercial applications.

4. CONCLUSION

According to DTA results obtained, simultaneous use of TiO_2 , ZrO_2 and CeO_2 as nucleating agents with various ratio is a the proper approach to obtain a high amount of the crystalline phase in bulk crystallization of glass-ceramics in $Li_2O-Al_2O_3-SiO_2$ system. The XRD results of different compositions showed revealed that the samples consisted of quartz as the minor phase, h-quartz (α -eucryptite s.s.) as the main phase. The most suitable nucleation temperature of the optimized samples were 680, 694 and 690°C, respectively. The Avrami constants (m, n) derived from the Marotta and Augis-Bennett, showed that glasses containing both ZrO_2 and TiO_2 nuclei represented bulk crystallization and specimens containing ZrO_2, TiO_2 and CeO_2 in the triple nuclei series represent two-dimensional bulk crystallization, which were confirmed by SEM analyses of microstructures. The minimum crystallization activation energy and maximum Avrami constant were obtained by combination of TiO_2 and ZrO_2 nucleating agents with amounts of 3Wt.% and 1Wt.%, respectively.

REFERENCES

1. Mc Milam P. W., "Glass-Ceramics", Harcourt Publishers LTD, 1979.
2. Strand Z., "Glass Ceramic Materials", Elsevier, 1986.
3. James P. F., "Glass ceramics: new compositions and uses", J. Non-Cryst. Sol., 1995, 181, 1–15.
4. Riello P., Canton P., "Nucleation and Crystallization Behavior of Glass-Ceramic Material in the LAS System of Interest for Their Transparency Properties", J. Non. Cryst. Solid. 2001, 288, 127-139.
5. Karmakarb K. P., "Crystallization Kinetics and Mechanism of Low-expansion Lithium Alumino silicate Glass-Ceramics by Dilatometry", J. Am. Ceram. Soc, 2002, 85, 2572-2574.
6. Beall, G. H., Pinckney L. R., "Nanophase Glass-Ceramics", J. Am. Ceram. Soc., 1999, 82, 5–16.
7. Arnault L., Gerland M., "Microstructural Study of two LAS-type Glass-Ceramics and Their Parent Glass", J. Mat. Sci., 2000, 35, 2331-2345.
8. Barbieri L., Leonell C., "Nucleation and Crystallization of a Lithium Alumino Silicate Glass", J. Am. Ceram. Soc., 1997, 80, 3077-3083.
9. Hsu J. Y., Speyer R. F., "Influences of Zirconia and Silicon Nucleating Agents on the Devitrification of $Li_2O-Al_2O_3-4SiO_2$ Glasses", J. Am. Ceram. Soc., 1990, 73, 3585–3593 (1990).
10. Maier, V., Mueller, G., "Mechanism of Oxide

- Nucleation in Lithium Alumino silicate Glass-Ceramics", *J. Am. Ceram. Soc.*, 1987, 70, 176-178.
11. Guo, X., Yang, H., "Nucleation and Crystallization Behavior of LAS System Glass-Ceramics Containing Little and no Fluorine", *J. Non-cryst. Solid.*, 351, 2133-2137.
 12. Sung, Y. M., Dunn, S. A., Koutsky, J. A., "The Effect of Boron and Titania Addition on the Crystallization and sintering Behaviour of $\text{Li}_2\text{O}-\text{Al}_2\text{O}_3-4\text{SiO}_2$ Glass", *J. Eur. Ceram. Soc.*, 1994, 14, 455-462.
 13. Guedes, M., Ferro, A. C., "Nucleation and Crystal Growth in Commercial LAS Compositions", *J. Eur. Ceram. Soc.*, 2001, 21, 1187-1194.
 14. Min, H. A., Ming, L. K., "Crystallization and Microstructural Changes in Fluorine Containing LAS Glasses", *Thermo. Act.*, 2004, 413, 53-55.
 15. Hu, A. M., Liang, K. M., Li, M., Mao, D. L., "Effect of Nucleation Temperatures and Time on Crystallization Behavior and Properties of $\text{Li}_2\text{O}-\text{Al}_2\text{O}_3-\text{SiO}_2$ Glasses", *Mater. Chem. Phys.*, 2006, 98, 430-433.
 16. Zheng, W., "Effect of Y_2O_3 Addition on Viscosity and Crystallization of the Lithium Aluminosilicate Glasses" *Therm. Chim. Act.*, 2007, 456, 69-74.
 17. Marotta A., "Activation Energy for The Crystallization of Glass from DDTA Curves", *J. Mat. Sci.*, 1982, 17, 105-108.
 18. Matusita, K., Sakka, S., "Study on Crystallization Kinetics in Glass By Differential Thermal Analysis", *Thermochim. Act.*, 1979, 334-351.
 19. Matusita, K., Sakka, S., " Kinetic Study on Crystallization of Glass By Differential Thermal Analysis-Criterion on Application of Kissinger Plot, *J. Non-cryst. Solids*, 1980, 38/39, 741-746.
 20. Ray, C. S., Day, D. E., "New Method for Determining the nucleation and Crystal-Growth Rates in Glasses", *J. Am. Ceram. Soc.*, 2000, 83, 865-872.
 21. Bach, H., "Low Thermal Expansion Glass-Ceramics", Springer Berlin, 1995.
 22. Barry, T. I., Clinton, D., Lay, L. L., Mercer, R. A., Miller, R. P., "The crystallization of glasses based on the eutectic compositions in the system $\text{Li}_2\text{O}-\text{Al}_2\text{O}_3-\text{SiO}_2$: part 2 lithium metasilicate β -eucryptite", *J. Mater. Sci.*, 1970, 5, 117-126.
 23. Hsu, J., Speyer, R. F., "Compression of the Effect of Titanium and Tantalum Oxide Nucleating Agents on the Crystallization of $\text{Li}_2\text{O}-\text{Al}_2\text{O}_3-\text{SiO}_2$ Glasses", *J. Am. Ceram. Soc.*, 1989, 72, 2334.
 24. Coon, D. N., Neilson, R. N., "Effect of MgO Addition on the Glass Transition Temperature of LAS Glasses", *J. Mat. Sci. Lett.*, 1998, 7, 33-35.
 25. Nocun, M., Baugajski W., "Effect of Y-PSZ Additive on the Structure , Thermal Behavior and Mechanical Properties of β -Spodumene Ceramics", *Key Eng. Mat.*, 1997, 32, 952-955.
 26. Matusita, K., Komatsu, T., Yokota, R., "Kinetics of Non-Isothermal Crystallization Process and Activation Energy for Crystal Growth in Amorphous Materials", *J. Mat. Sci.*, 1984, 19, 291-296.
 27. Hu, A. M., Liang, K. M., "Phase Transformation of $\text{Li}_2\text{O}-\text{Al}_2\text{O}_3-\text{SiO}_2$ Glasses with CeO_2 Addition", *Ceram. Int.*, 2005, 31, 11-14.
 28. Kinckerbocker, S., Tuzzolo, M. R., "Sinterable β -Spodumene Glass-Ceramics", *J. Am. Ceram. Soc.*, 1989, 72, 1873-1879.